ESKİŞEHİR TECHNICAL UNIVERSITY JOURNAL OF SCIENCE AND TECHNOLOGY
A- APPLIED SCIENCES AND ENGINEERING

2019, Vol: 20, pp. 105 -113, DOI: 10.18038/estubtda.644026

THEORETICAL AND EXPERIMENTAL INFRARED SPECTRUM ANALYSIS OF 1-ETHYL-3-METHYLIMIDAZOLIUM CATION

Nihal KUŞ*, Saliha ILICAN

Department of Physics, Science Faculty, Eskisehir Technical University, 26470, Eskisehir, Turkey

ABSTRACT

In this study, molecular structure of 1-ethyl-3-methylimidazolium cation (EMIM$^+$) was undertaken at the DFT(B3LYP)/6-311++G(2d,2p) level of approximation using the GAUSSIAN 09 suit of programs. EMIM has two conformers (EMIM-1 and EMIM-2) with minimum energies. EMIM-1 and EMIM-2 were found C1 (double degenerated by-symmetry form) and Cs symmetries, respectively. Normal coordinate analyses were performed with the BALGA program. Experimental infrared spectra of EMIM were obtained by increasing temperature (between room temperature and 150°C) and compared with calculations. Assignment of the spectra and normal coordinate analyses to characterize the vibrations in EMIM conformers were undertaken. p-electron delocalization through the aromaticity index Harmonic Oscillator Measure of Aromaticity (HOMA) of EMIM calculated using Kruszewski and Krygowski definations.

Keywords: 1-Ethyl-3-methylimidazolium, IR spectra, DFT, HOMA

1. INTRODUCTION

Interest in ionic liquids (ILs), also called molten salt, has increased recently. It has been used frequently in the extraction of new chemicals, in the production of fuel cells, batteries and new composite materials. Most of the uses in these areas were unpredictable for their presumed non-volatility [1, 2]. However, many ionic liquids are now known to allow for distillation under reduced pressure without decomposition [3-5]. This fact has created a new field of application for these compounds in gas-phase processes. The most important question raised by the recognition of the demonstrated measurable volatility of ILs is that they depend on the nature of the various species in the gas phase. In a recent study, J.P. Leal et al. [3] reported that the neutral ion pairs do not have a detectable concentration of aprotic ILs at low pressure and above 474 K, whereas protic ILs were found to consist in the gas phase as separated neutral molecules. Nevertheless, the nature of the species in the gas phase resulting from evaporation of ILs are still controversial. For example, earlier mass spectrometric studies [6-7] were at least somewhat in contradiction to the results described in ref. [3].

In the present study, conformational analysis on 1-ethyl-3-methylimidazolium cation (EMIM$^+$) (Figure 1) has been carried out using density functional theory (DFT) with the B3LYP hybrid functional and the 6-311++G(2d,2p) basis set, and the dependence of vibrational properties with molecular conformation investigated. Besides the theoretical studies, EMIM has also been studied by FT-IR spectroscopy in a KBr matrix, at different temperature (room temp. to 150°C). From results of the DFT calculation, EMIM-1 and EMIM-2 were found C1 (double degenerated by-symmetry form) and Cs symmetries. Normal coordinate analyses were performed with the BALGA program. Spectrum determination and normal coordinate analyses were performed to characterize the vibrations in EMIM. p-Electron delocalization through the index of aromaticity Harmonic Oscillator Measure of Aromaticity (HOMA) for EMIM calculated using Kruszewski and Krygowski definitions. Matrix-isolation studies on this compound are on the way, in order to evaluate the vibrational characteristics of the isolated molecules of the compound and study its uni-molecular photochemistry.

---

*Corresponding Author: nkus@eskisehir.edu.tr
Received: 11.10.2019 Published: 16.12.2019

2. MATERIAL AND METHODS

Theoretical studies were undertaken at the DFT(B3LYP)/6-311++G(2d,2p) level of approximation using the GAUSSIAN 09 suit of programs. Normal coordinate analyses were performed with the BALGA program. The detailed definition is given in the potential energy distribution (PED). The IR spectra of EMIM-1 and EMIM-2 were taken on a FT-IR BOMEM MB 104 with ZnSe optics. The resolution was set to 4cm^{-1} and temperature was varied systematically using a thermoelectrically heated device. Temperature variation studies were undertaken using a SPECAC infrared variable temperature cell connected to a temperature digital controller (Red Lions). The estimated uncertainty in temperature is ±2°C.

3. RESULTS AND DISCUSSION

Minimum energies on stable state EMIM-1 and EMIM-2 cation forms (Figure 1) calculated using DFT(B3LYP)/6-311++G(2d,2p) level of approximation. EMIM-1 relative electronic energy E(UB3LYP) was found to be more stable than the EMIM-2 by 2.3 kJ mol^{-1} (Table 1). EMIM-1 and EMIM-2 are C1 (double degenerated by-symmetry form) and Cs. In agreement with previously reported ab initio and DFT(B3LYP)/6-31G* calculations [8, 9].

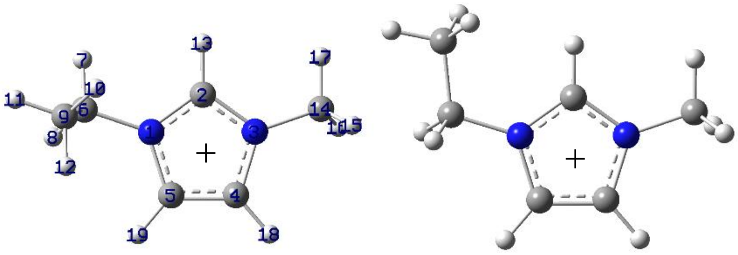

EMIM–1

EMIM–2

Figure 1. Conformers of EMIM calculated by DFT(B3LYP)/6-311++G(2d,2p) level.

Table 1. Calculated relative energies of EMIM-1 and EMIM-2 using DFT(B3LYP)/6-311++G(2d,2p) level

	ΔE(UB3LYP) kJ mol^{-1}	**Δ(E+ZPV) kJ mol^{-1}**	**ΔG kJ mol^{-1}**
EMIM-1	0	0	0
EMIM-2	2.33	2.46	1.48

Figure 2 presents the potential energy profile for internal rotation around the N-CH2 bond and shows steps for interconversion between the two minimum energies of EMIM. Transition states form of EMIM are also shown in Figure 2. Calculated barrier energy from EMIM-1 to EMIM-2 is 5.2 kJ mol^{-1} and in the opposite direction is 2.8 kJ mol^{-1}.

Table 2. Calculated [B3LYP/6-311++G(2d,2p) bond lengths for 1-Ethyl-3-Methylimidazolium cation [EMIM]+ (atom numbering as in Figure 1).

Bond lengths/ Å	**EMIM-1**	**EMIM-2**	**B3LYP/ 6-31G* [10]**	**X-RAY**		
				[11]	**[11]**	**[12]**
N1-C2	1.334	1.334	1.335	(1.327)	(1.324)	(1.324)
N1−C5	1.379	1.380	1.385	(1.376)	(1.374)	(1.356)
N1−C6	1.481	1.486	1.480	(1.489)	(1.475)	(1.485)
N3=C2	1.335	1.335				
C2 – H13	1.075	1.074				
N3 – C4	1.380	1.379	1.385	(1.367)	(1.368)	(1.366)
N3 – C14	1.468	1.468	1.467	(1.449)	(1.462)	(1.463)
C4 =C5	1.359	1.358	1.363	(1.352)	(1.322)	(1.330)
C4 – H18	1.074	1.074				
C5 – H19	1.074	1.074				
C6 – H7	1.088	1.089				
C6 – H8	1.088	1.089				
C6 – C9	1.523	1.518	1.527	(1.472)	(1.475)	(1.505)
C9 – H10	1.089	1.090				
C9 – H11	1.089	1.088				
C9 – H12	1.089	1.090				
C14 – H15	1.087	1.087				
C14 – H16	1.087	1.087				
C14 – H17	1.085	1.085				

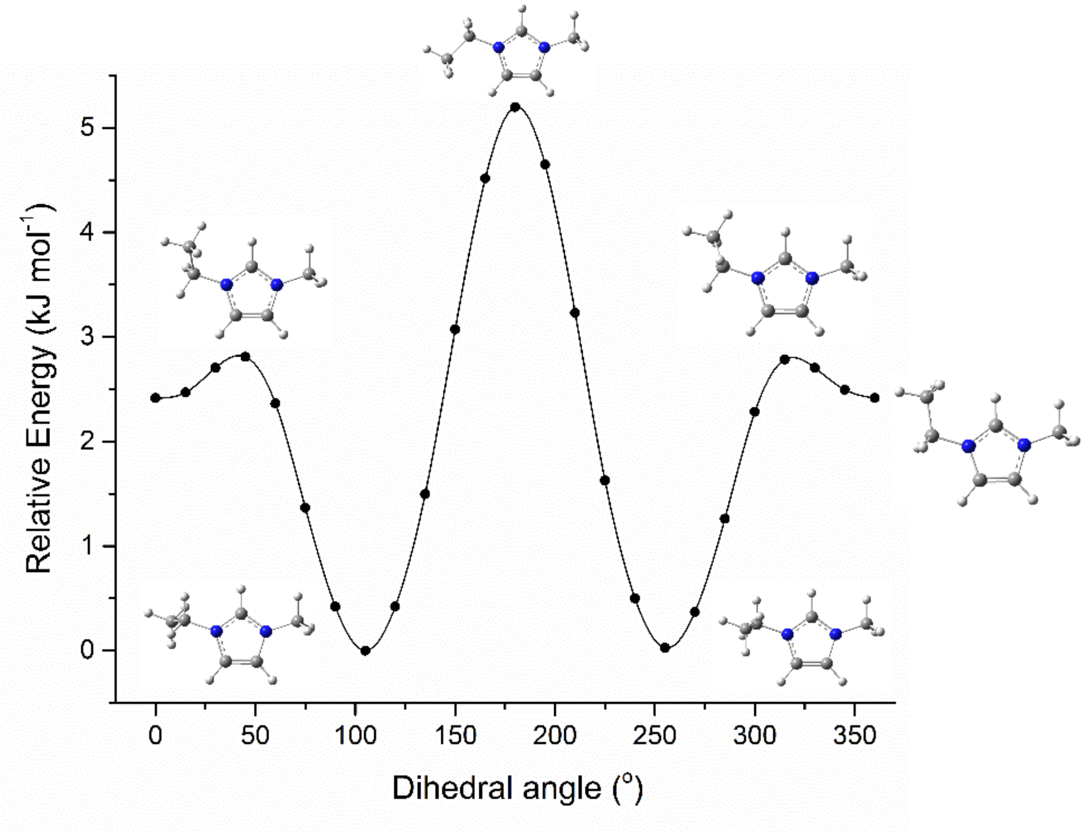

Figure 2. Calculated potential energy profile for EMIM-1 to EMIM-2 interconversion with B3LYP/6-311++G(d,p) (atom numbers are given in Figure 1)

Table 3. Internal coordinates used in the normal modes analysis for EMIM+ (atom numbering as in Figure 1).

Coordinate	Definition	Symmetry	Approximate description
S_1	$r_{1,2}$	A'	ν(N1-C2)
S_2	$r_{2,3}$	A'	ν(N3=C2)
S_3	$r_{3,4}$	A'	ν(N3-C4)
S_4	$r_{4,5}$	A'	ν(C4=C5)
S_5	$r_{5,1}$	A'	ν(N1-C5)
S_6	$r_{6,7} + r_{6,8}$	A'	$\nu(\mathrm{CH2})_{s}$
S_7	$r_{6,7} - r_{6,8}$	A'	$\nu(\mathrm{CH2})_{as}$
S_8	$r_{9,11} + r_{9,10} + r_{9,12}$	A'	$\nu(\mathrm{CH3})_{s(et)}$
S_9	$2\, r_{9,11} - r_{9,10} - r_{9,12}$	A'	$\nu(\mathrm{CH3})_{as'(et)}$
S_{10}	$r_{9,10} - r_{9,12}$	A'	$\nu(\mathrm{CH3})_{as''(et)}$
S_{11}	$r_{14,16} + r_{14,17} + r_{14,15}$	A'	$\nu(\mathrm{CH3})_{s}$
S_{12}	$2\, r_{14,16} - r_{14,17} - r_{14,15}$	A'	$\nu(\mathrm{CH3})_{as'}$
S_{13}	$r_{14,17} - r_{14,15}$	A'	$\nu(\mathrm{CH3})_{as''}$
S_{14}	$r_{2,13}$	A'	ν(C2-H)
S_{15}	$r_{4,18}$	A'	ν(C4-H)
S_{16}	$r_{5,19}$	A'	ν(C5-H)
S_{17}	$r_{3,14}$	A'	ν(N3-C14)
S_{18}	$r_{1,6}$	A'	ν(N1-C6)
S_{19}	$r_{6,9}$	A'	ν(C6-C9)
S_{20}	$\beta_{11,12,9} + \beta_{12,10,9} + \beta_{10,11,9} - \beta_{11,6,9} - \beta_{12,6,9} - \beta_{10,6,9}$	A''	$\delta(\mathrm{CH3})_{s(et)}$
S_{21}	$2\beta_{11,12,9} - \beta_{12,10,9} - \beta_{10,11,9}$	A''	$\delta(\mathrm{CH3})_{as'(et)}$
S_{22}	$\beta_{12,10,9} - \beta_{10,11,9}$	A''	$\delta(\mathrm{CH3})_{as''(et)}$
S_{23}	$2\beta_{11,6,9} - \beta_{12,6,9} - \beta_{10,6,9}$	A''	$\gamma(\mathrm{CH3})'_{(et)}$
S_{24}	$\beta_{12,6,9} - \beta_{10,6,9}$	A''	$\gamma(\mathrm{CH3})''_{(et)}$
S_{25}	$\beta_{16,15,14} + \beta_{15,17,14} + \beta_{17,16,14} - \beta_{16,3,14} - \beta_{15,3,14} - \beta_{17,2,14}$	A''	$\delta(\mathrm{CH3})_{s}$
S_{26}	$2\beta_{16,15,14} - \beta_{15,17,14} - \beta_{17,16,14}$	A''	$\delta(\mathrm{CH3})_{as'}$
S_{27}	$\beta_{15,17,14} - \beta_{17,16,14}$	A''	$\delta(\mathrm{CH3})_{as''}$
S_{28}	$2\beta_{16,3,14} - \beta_{15,3,14} - \beta_{17,2,14}$	A''	γ(CH3)′
S_{29}	$\beta_{15,3,14} - \beta_{17,2,14}$	A''	γ(CH3)″
S_{30}	$5\beta_{8,6,7} - \beta_{8,6,1} - \beta_{7,6,1} - \beta_{8,6,9} - \beta_{7,6,9} - \beta_{9,6,1}$	A''	sc(CH_2)
S_{31}	$4\beta_{9,6,1} - \beta_{8,6,1} - \beta_{7,6,1} - \beta_{8,6,9} - \beta_{7,6,9}$	A''	sc(N1-C9)
S_{32}	$\beta_{8,6,1} - \beta_{7,6,1} + \beta_{8,6,9} - \beta_{7,6,9}$	A''	r(CH_2)
S_{33}	$\beta_{8,6,1} + \beta_{7,6,1} - \beta_{8,6,9} - \beta_{7,6,9}$	A''	w(CH_2)
S_{34}	$\beta_{8,6,1} - \beta_{7,6,1} - \beta_{8,6,9} + \beta_{7,6,9}$	A''	t(CH_2)
S_{35}	$\beta_{1,19,5} - \beta_{4,19,5}$	A''	δ(C5-H)
S_{36}	$\beta_{5,18,4} - \beta_{3,18,4}$	A''	δ(C4-H)
S_{37}	$\beta_{1,13,2} - \beta_{3,13,2}$	A''	δ(C2-H)
S_{38}	$\beta_{6,2,1} - \beta_{6,5,1}$	A''	δ(N1-C6)
S_{39}	$\beta_{14,4,3} - \beta_{14,2,3}$	A''	δ(N3-C14)
S_{40}	$-0.309\beta_{3,5,4} - 0.809\beta_{2,4,3} + 0.809\beta_{4,1,5} + 0.309\beta_{1,3,2} + \beta_{5,2,1}$	A''	δ ring
S_{41}	$-1.118\beta_{2,4,3} + 1.118.\beta_{4,1,5} -1.809\beta_{1,3,2} + 1.809\beta_{5,2,1}$	A''	δ ring′
S_{42}	$\tau_{16,14,3,4} + \tau_{5,4,3,14}$	A''	τ(N1-C6)
S_{43}	$\tau_{5,1,6,8} + \tau_{4,5,1,6}$	A''	τ(N3-C14)
S_{44}	$\tau_{1,6,9,10}$	A''	τ(C6-C9)
S_{45}	$-0.309\tau_{3,2,1,5} - 0.809\tau_{4,3,2,1} + 0.809\tau_{2,1,5,4} + 0.309\tau_{5,4,3,2} + \tau_{1,5,4,3}$	A''	τ ring
S_{46}	$-1.118\tau_{4,3,2,1} + 1.118\tau_{2,1,5,4} + -1.809\tau_{5,4,3,2} + 1.809\tau_{1,5,4,3}$	A''	τ ring′
S_{47}	$\gamma_{19,4,5,1}$	A''	γ(C5-H)
S_{48}	$\gamma_{18,3,4,5}$	A''	γ(C4-H)
S_{49}	$\gamma_{5,2,6,1}$	A''	γ(N1-C6)
S_{50}	$\gamma_{13,1,2,3}$	A''	γ(C2-H)
S_{51}	$\gamma_{14,2,3,4}$	A''	γ(N3-C14)

$r_{i,j}$ is the distance between atoms A_i and A_j; $\beta_{i,j,k}$ is the angle between vectors A_kA_i and A_kA_j; $\tau_{i,j,k,l}$ is the dihedral angle between the plane defined by A_i, A_j, A_k and the plane defined by A_j, A_k, A_l atoms; $\gamma_{i,j,k,l}$ is the angle between the vector A_kA_i and the plane defined by atoms A_j, A_k, A_l;
ν, stretching, δ, bending, γ, out-of-plane, τ, torsion, sc, scissoring, r, rocking, w, wagging, r, rocking, t, twisting, s, symmetric, as, asymmetric.

Table 4. Results of the normal coordinate analyses for most stable conformer EMIM-1.

Approx. Desc.[a]	Sym.	Calc.Freq.[b]	Int.[c]	PED[d]
ν(C2-H)	A′	3300	9.0	ν(C2-H)(83.8)
ν(C5-H)	A′	3294	31.7	ν(C5-H)(44.5) + ν(C4-H)(39.0) + ν(C2-H)(15.3)
ν(C4-H)	A′	3278	16.4	ν(C4-H)(52.6) + ν(C5-H)(46.9)
ν(CH3)$_{as''}$	A′	3170	0.3	ν(CH3)$_{as''}$ (74.4) + ν(CH3)$_{as'}$ (24.8)
ν(CH3)$_{as'}$	A′	3155	0.1	ν(CH3)$_{as'}$ (75.1) + ν(CH3)$_{as''}$ (25.0)
ν(CH3)$_{as'(et)}$	A′	3129	2.6	ν(CH3)$_{as'(et)}$ (95.9)
ν(CH3)$_{as''(et)}$	A′	3128	6.6	ν(CH2)$_{as}$ (55.6) + ν(CH3)$_{as''(et)}$ (44.6)
ν(CH2)$_{as}$	A′	3106	1.9	ν(CH3)$_{as''(et)}$ (55.6) + ν(CH2)$_{as}$ (44.7)
ν(CH3)$_{s}$	A′	3078	3.3	ν(CH3)$_{s}$ (98.5)
ν(CH2)$_{s}$	A′	3077	3.4	ν(CH2)$_{s}$ (97.4)
ν(CH3)$_{s(et)}$	A′	3051	3.7	ν(CH3)$_{s(et)}$ (94.9)
ν(C4=C5)	A′	1607	15.1	ν(C4=C5)(38.3) + ν(N3=C2)(16.3) + δ(C5-H)(12.7)
δ(C2-H)	A′′	1601	53.0	ν(C4=C5)(30.4) + δ(C2-H)(16.4) + ν(N1-C2)(14.0)
δ(CH3)$_{as'}$	A′′	1515	7.9	δ(CH3)$_{as'}$ (66.9)
δ(CH3)$_{as''(et)}$	A′′	1515	3.2	sc(CH2)(33.5) + δ(CH3)$_{as''(et)}$ (30.1) + δ(CH3)$_{as'}$ (10.8) + δ(CH3)$_{as'\text{-}A}$ (10.0)
sc(CH2)	A′′	1507	5.1	sc(CH2)(47.8) + δ(CH3)$_{as''\text{-}A}$ (31.4) + δ(CH3)$_{as'\text{-}A}$ (10.3)
δ(CH3)$_{as'(et)}$	A′′	1505	12.0	δ(CH3)$_{as'(et)}$ (69.1) + δ(CH3)$_{as''(et)}$ (21.4)
δ(CH3)$_{as''}$	A′′	1491	14.8	δ(CH3)$_{as''}$ (88.7)
δ(CH3)$_{s}$	A′′	1470	4.0	δ(CH3)$_{s}$ (86.6)
w(CH2)	A′′	1442	12.0	δ(CH3)$_{s(et)}$ (31.7) + w(CH2)(20.8)
δ(CH3)$_{s(et)}$	A′′	1427	7.6	δ(CH3)$_{s(et)}$ (64.4) + w(CH2)(12.9)
ν(N3-C4)	A′	1409	2.5	ν(N3-C2)(24.8) + ν(N3-C4)(21.2) + δ(CH3)$_{as'}$ (12.2)
ν(N1-C2)	A′	1361	26.6	w(CH2)(27.5) + ν(N1-C2)(17.8) + ν(N1-C6)(10.0)
ν(N1-C5)	A′	1327	7.9	ν(N1-C5)(15.9) + ν(N3-C14)(14.2) + ν(N3-C4)(14.1) + δ(C5-H)(9.8)
t(CH$_2$)	A′′	1326	1.5	t(CH$_2$)(87.4) + γ(CH3)′′$_{(et)}$ (11.2)
δ(C4-H)	A′′	1288	10.4	δ (C2-H)(30.9) + δ(C4-H)(16.0) + δ(C5-H)(14.8)
δ(C2-H)	A′′	1170	100.6	δ(C2-H)(28.4) + ν(N1-C6)(16.2) + ν(N3-C14)(12.7) + ν(N1-C5)(9.8) + δ(C4-H)(9.7)
r(CH$_2$)	A′′	1167	1.3	r(CH$_2$)(43.8) + γ(CH3)′′$_{(et)}$ (39.0)
γ(CH3)′	A′′	1154	0.2	γ(CH3)′ (61.2) + γ(CH3)′′ (19.8) + δ(CH3)$_{as''}$ (9.7)
δ(C5-H)	A′′	1127	11.2	δ(C5-H)(34.8) + δ(C4-H)(25.9) + ν(C4=C5)(19.2) + ν(N1-C5)(9.6)
γ(CH3)′$_{(et)}$	A′′	1107	0.3	γ(CH3)′$_{(et)}$ (34.7) + ν(C6-C9)(13.3) + sc(N1-C9)(9.7)
γ(CH3)′′	A′′	1102	3.5	γ(CH3)′′ (33.1) + γ(CH3)′ (11.0) + γ(CH3)′$_{(et)}$ (10.5)
δ ring	A′′	1049	0.4	ν(N1-C5)(27.3) + δ ring (19.4) + ν(C6-C9)(18.8)
δ ring′	A′′	1038	1.4	δ ring′ (46.2) + ν(N3-C4)(17.0)
ν(C6-C9)	A′	975	1.7	ν(C6-C9)(39.2) + γ(CH3)′$_{A}$ (26.1) + δ ring (18.3)
γ(C5-H)	A′′	879	0.1	γ(C5-H)(57.3) + γ(C4-H)(52.2)
γ(C2-H)	A′′	845	37.3	γ(C2-H)(72.5) + γ(C4-H)(9.9)
γ(CH3)′′$_{(et)}$	A′′	809	0.9	r(CH$_2$)(43.3) + γ(CH3)′′$_{(et)}$ (32.6) + γ(C2-H)(12.1)
γ(C4-H)	A′′	753	28.4	γ(C4-H)(43.0) + γ(C5-H)(41.1) + γ(C2-H)(15.4)
ν(N3-C14)	A′	706	7.0	δ ring′ (30.6) + ν(N3-C14)(28.2) + ν(N1-C6)(17.0)
τ ring′	A′′	639	18.7	τ ring′ (95.9)
τ ring	A′′	635	2.7	τ ring (100.4)
ν(N1-C6)	A′	591	1.3	ν(N1-C6)(22.8) + δ ring (21.3) + ν(N3-C14)(20.8)
sc(N1-C9)	A′′	447	0.8	δ(N1-C6)(29.5) + δ(N3-C14)(17.3) + sc(N1-C9)(15.1) + ν(N1-C6)(10.8) + ν(C6-C9)(10.7)
δ(N3-C14)	A′′	355	0.5	δ(N3-C14)(56.3) + sc(N1-C9)(26.7)
τ(C6-C9)	A′′	299	0.2	τ(C6-C9)(80.2) + γ(N1-C6)(18.4)
γ(N3-C14)	A′′	247	0.7	γ(N3-C14)(62.8) + γ(N1-C6)(18.2) + τ(C6-C9)(14.3)
δ(N1-C6)	A′′	187	0.6	δ(N1-C6)(53.4) + sc(N1-C9)(25.8) + δ(N3-C14)(14.3)
γ(N1-C6)	A′′	168	3.5	γ(N1-C6)(60.9) + γ(N3-C14)(23.5)
τ(N1-C6)	A′′	72	0.1	τ(N1-C6)(97.0)
τ(N3-C14)	A′′	31	0.3	τ(N3-C14)(104.6)

[a] ν, stretching, δ, bending, γ, out-of-plane, τ, torsion, sc, scissoring, r, rocking, w, wagging, r, rocking, t, twisting, s, symmetric, as, asymmetric. See Table 3 for definition of symmetry coordinates and Figure 1 for atom numbering. [b] Frequencies: cm^{-1}. [c] Intensities: km mol^{-1}. [d] The description is given in the PED form and higher than 10 % are included.

Table 5. Experimental and calculated (using B3LYP/6-311++G(2d,2p) basis set) frequencies (cm^{-1}) for EMIM^{+}.

Approximate description	**Calculated (present)**	**B3LYP (6-31G*) [10]**	**Exp. IR [10, 11]**	**Exp. IR (KBr) [11]**	**Exp. IR (present)**
ν(C2-H)	3300				
ν(C5-H)	3294				
ν(C4-H)	3278				
ν(CH3)$_{as''}$	3170	3168	3166	3168	
ν(CH3)$_{as'}$	3155	3162		3133	3133
ν(CH3)$_{as'(et)}$	3129		3125		
ν(CH3)$_{as''(et)}$	3128				
ν(CH2)$_{as}$	3106				
ν(CH3)$_{s}$	3078				
ν(CH2)$_{s}$	3077				
ν(CH3)$_{s(et)}$	3051				3060
ν(C4=C5)	1607	1582	1619	1613	
δ(C2-H)	1601		1576	1572	1570
δ(CH3)$_{as'}$	1515				
δ(CH3)$_{as''(et)}$	1515				
sc(CH2)	1507				
δ(CH3)$_{as'(et)}$	1505				
δ(CH3)$_{as''}$	1491				
δ(CH3)$_{s}$	1470	1464	1462	1466	1468
w(CH2)	1442	1447	1458	1452	1454
δ(CH3)$_{s(et)}$	1427	1423		1426	
ν(N3-C4)	1409	1409		1402	1391
ν(N1-C2)	1361	1361		1360	
ν(N1-C5)	1327		1337	1335	1335
t(CH$_2$)	1326				
δ(C4-H)	1288	1288	1286	1295	1299
δ(C2-H)	1170			1170	1171
r(CH$_2$)	1167		1062		
γ(CH3)′	1154	1153			
δ(C5-H)	1127	1129		1133	
γ(CH3)′$_{(et)}$	1107	1117		1118	
γ(CH3)″	1102	1102		1094	1087
δ ring	1049	1026			
δ ring′	1038			1034	1026
ν(C6-C9)	975		960	955	959
γ(C5-H)	879	937	896	882	
γ(C2-H)	845	851	849	858	863
γ(CH3)″$_{(et)}$	809	815	805	810	
γ(C4-H)	753	787	758	748	750
ν(N3-C14)	706		702	701	701
τ ring′	639			647	645
τ ring	635	620	623	637	619
ν(N1-C6)	591	580	598	590	596
sc(N1-C9)	447	425	423	458	n.o
δ(N3-C14)	355	375	354	362	n.o
τ(C6-C9)	299	286	294		n.o
γ(N3-C14)	247	229	243		n.o
δ(N1-C6)	187				n.o
γ(N1-C6)	168				n.o
τ(N1-C6)	72				n.o
τ(N3-C14)	31				n.o

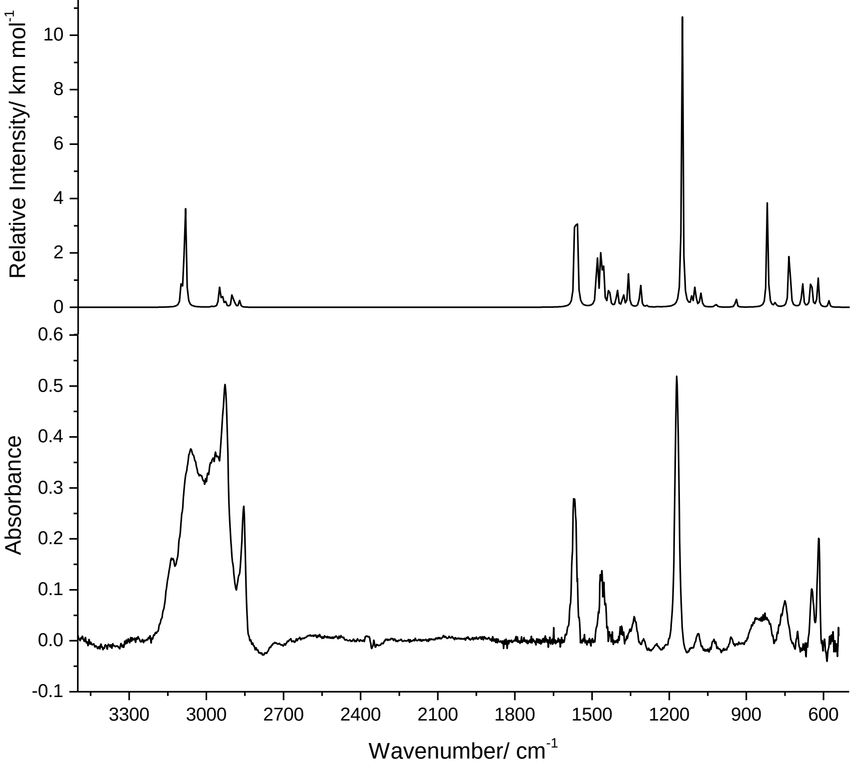

Figure 3. Bottom: Experimental Infrared spectrum (3500-580 cm^{-1} region) of EMIM at 125 °C. Top: Calculated infrared spectrum of EMIM-1 using B3LYP/6-311++G(2d,2p) level. In the calculated spectrum, wavenumbers were scaled by a factor of 0.940 in the 3500–2500 cm^{-1} range and with a factor of 0.978 in the range below 2500 cm^{-1} and the bands were simulated by Lorentzian functions centered at the calculated wavenumbers and with a full width at half maximum (FWHM) equal to 6 cm^{-1}.

Previous experimental and theoretically vibrational spectroscopy results for the compound have been reported [13-15]. Calculated infrared spectrum for the isolated molecule's most stable conformer (top) fit very nicely the experimental data. EMIM was studied both dispersed in KBr matrix and as a thin film. The spectra of the compounds practically do not change with temperature (from room temperature up to 150°C), in particular the spectra of the liquid and crystalline phases are identical, indicating the molecular environment is very similar in these two phases.

From the ring bond lengths, it is possible to evaluate the level of p-electron delocalization through the aromaticity index Harmonic Oscillator Measure of Aromaticity (HOMA), defined by Kruszewski and Krygowski [16-18],

$$HOMA = 1 - \frac{\alpha}{n}\sum_{i=1}^{n}(R_{opt} - R_i)^2 \qquad (1)$$

where n is the number of bonds considered belong to C-C and C-N bonds, and α is the empirical constant, which are 257.7 and 93.52, respectively. If HOMA is equal to zero, it can be called a non-aromatic system; however, a fully aromatic system occurs when HOMA is equal to one. In this equation R_i gives the length of the running bond (Table 2). The reference values R_{opt} for the C-C bond is 1.3963 Å, whereas for the C-N bond it is taken as 1.3288 Å [19]. The obtained HOMA index for both EMIM-

1 and EMIM-2 (0.520), reveals the relatively low degree of aromaticity of the imidazolium ring in these compounds, which is similar to the one of the α-pyrone ring (0.526) in coumarin [20].

4. CONCLUSIONS

$EMIM^+$ was investigated experimentally using infrared spectroscopy and supported by DFT(B3LYP)/6-311++G- (2d,2p) calculations. As results of calculations, it was indicated that the molecule has two conformers (EMIM-1 and EMIM-2). The $EMIM^+$ molecule was found to be in both liquid and crystal phase environments. The IR spectra of the compound in the liquid and crystalline phase as a function of temperature were unchanged (from room temperature to 150°C). When the temperature-dependent spectra were recorded, sharp and dense spectra were observed at high temperature (at 125°C). Assignment of the spectra and normal coordinate analyses to characterize the vibrations in EMIM-1 were undertaken. It was found that the calculated PED and experimental spectra were in agreement and gave better results in high level calculations. HOMA index for both conformations of EMIM were the similar, and it was found to be 0.52.

ACKNOWLEDGMENT

This work was supported by the Eskisehir Technical University Commission of Research Project under grant no: 19ADP130.

REFERENCES

[1] Rogers RD, Seddon, KR, Eds., Ionic Liquids IIIA: Fundamentals, Progress, Challenges, and Opportunities - Properties and Structure; Ionic Liquids IIIB: Fundamentals, Progress, Challenges, and Opportunities - Transformations and Processes, American Chemical Society, Washington, DC, 2005.

[2] Rogers RD, Seddon KR,Volkov S, Eds., Green Industrial Applications of Ionic Liquids, Kluwer, Dordrecht, 2002.

[3] Leal JP, Esperança JMSS, Minas da Piedade ME, Canongia Lopes JN, Rebelo LPN, Seddon KR. The Nature of Ionic Liquids in the Gas Phase. J Phys Chem A 2007; 111: 6176-6182.

[4] Earle MJ, Esperança JMSS, Gilea MA, Lopes JNC, Rebelo LPN, Magee JW, Seddon KR, Widegren JA. The distillation and Volatility of Ionic Liquids. Nature 2006; 439: 831-834.

[5] Paulechka YU, Zaitsau DH, Kabo GJ, Strechan AA. Vapor Pressure and Thermal Stability of Ionic Liquid 1-Butyl-3-methylimidazolium Bis(trifluoromethylsulfonyl)amide. Thermochim Acta 2005; 439: 158-160.

[6] A.-Sada AK, Elaiwi AE, Greenway AM, Seddon KR. Evidence for the Clustering of Substituted Imidazolium Salts via Hydrogen Bonding under the Conditions of Fast Atom Bombardment Mass Spectrometry. Eur J Mass Spectrom 1997; 3: 245-247.

[7] Alfassi ZB, Huie RE, Milman BL, Neta P. Electrospray Ionization Mass Spectrometry of Ionic Liquids and Determination of their Solubility in Water. Anal Bioanal Chem 2003; 377: 159-164.

[8] Turner EA, Pye CC, Singer RD. Use of ab initio calculation towards the rational design of room temperature ionic liquids. J Phys Chem A 2003; 107: 2277-2288.

[9] Katsyuba SA, Zvereva EE, Vidiš A, Dyson P J. Application of density functional theory and vibrational spectroscopy toward the rational design of ionic liquids. J Phys Chem A 2007; 111: 352-370.

[10] Katsyuba SA, Dyson PJ, Vandyukova EE, Chernova AV, Vidis A. Molecular Structure, Vibrational Spectra, and Hydrogen Bonding of the Ionic Liquid 1-Ethyl-3-methyl-1H-imidazolium Tetrafluoroborate. Helvetica Chem Acta 2004; 87: 2556-2565.

[11] Elaiwi A, Hitchcock P B, Seddon KR, Srinivasan N, Tan Y-M, Welton T, Zora, JA. Hydrogen bonding in imidazolium salts and its implications for ambient-temperature halogenoaluminate(III) ionic liquids. J Chem Soc Dalton Trans 1995; 21: 3467-3472.

[12] Fuller J, Carlin RT, De Long H C, Haworth D. Structure of 1-ethyl-3-methylimidazolium hexafluorophosphate: model for room temperature molten salts. J Chem Soc Chem Commun 1994; 3: 299-300.

[13] Pernak J, Sobaszkiewicz K, Mirska I. Anti-microbial activities of ionic liquids. Green Chem 2003; 5: 52-56.

[14] Scammels PJ, Scott JL, Singer RD. Ionic liquids: the neglected issues. Aust J Chem 2005; 58: 155-169.

[15] Gathergood N, Scammells PJ. Design and Preparation of Room-Temperature Ionic Liquids Containing Biodegradable Side Chains. Aust J Chem 2002; 55: 557-560.

[16] Kruszewski J, Krygowski TM. Definition of aromaticity basing on the harmonic oscillator model. Tet Lett 1972; 13: 3839-3942.

[17] Krygowski TM. Crystallographic studies of inter- and intramolecular interactions reflected in aromatic character of .pi.-electron systems. J Chem Inform. Comp. Sci., 1993, 33, 70-78.

[18] Krygowski TM, Cyranski M. Separation of the energetic and geometric contributions to the aromaticity of π-electron carbocyclics. Tetrahedron 1996; 52: 1713-1722.

[19] Morrison CA, Smart BA, Rankin DWH, Robertson HE, Pfeffer M, Bodenmüller W, Ruber R, Macht B, Ruoff A, Typke V. Molecular Structure of 1,3,5-Triazine in Gas, Solution, and Crystal Phases and by ab Initio Calculations. J Phys Chem A 1997; 101: 10029-10038.

[20] Kuş N, Breda S, Reva ID, Tasal E, Ogretir C, Fausto R. FTIR spectroscopic and theoretical study of the photochemistry of matrix-isolated coumarin. Photochem Photobiol 2007; 83: 1237-1253.